Int. J. Electrochem. Sci., 7 **(2012)** 9465 - 9477

International Journal of
ELECTROCHEMICAL
SCIENCE
www.electrochemsci.org

Formation of $Cr_{23}C_6$ during the Sensitization of AISI 304 Stainless Steel and its Effect to Pitting Corrosion

Mohd Warikh Abd Rashid, Miron Gakim, Zulkifli Mohd Rosli, Mohd Asyadi Azam[*]

Engineering Materials Department, Faculty of Manufacturing Engineering, Universiti Teknikal Malaysia Melaka (UTeM), Hang Tuah Jaya, 76100 Durian Tunggal, Melaka, Malaysia.
[*]E-mail: asyadi@utem.edu.my

Received: 10 July 2012 / *Accepted:* 29 August 2012 / *Published:* 1 October 2012

The metallic carbide precipitation was observed after the sensitization of AISI 304 stainless steel specimens in neutral flame by using oxy-fuel and slowly cooled in the air. Correlation between corrosion and X-Ray Diffraction (XRD) shows that the enrichment of $Cr_{23}C_6$ in the microstructure of AISI 304 worsens the pitting corrosion resistance properties as the sensitization time increases from 5 to 60 s. However, the precipitation dissolved and corrosion resistance properties improved after the specimens treated in solution quenching treatment at 1130 ^{o}C, soaked from 24 – 120 min, then rapidly cooled in water.

Keywords: Stainless Steel, Alloy, Pitting Corrosion, Polarization, X-ray diffraction.

1. INTRODUCTION

The austenitic stainless steels have high corrosion resistance ability because of high chromium (Cr) content and also nickel (Ni) addition in its alloy. Because of this advantage, for example, the conducting stainless steel foils have been used as current collectors in nanomaterials based electrochemical or energy device research [1 – 2]. When austenitic stainless is exposed into the corrosive aqueous solution, chromium oxide enriches at the metal-film interface due to the formation of passive layer, which is primarily attribute its high corrosion properties [3 – 6]. Thus, austenitic stainless steels were developed for the application in both mild and severe corrosion environment. However, under the action of aggressive ions, such chloride anion in seawater, local breakdown of passivity occurs, mainly at the sites of local heterogeneities, causing pitting corrosion.

Microstructure of austenitic stainless steels also is an important factor that attributing its pitting corrosion resistance. Generally, fully austenitic structure has the lowest susceptibility to pitting

corrosion attack [7]. Many studies evidenced that, austenitic structure is reducing susceptibility to pitting corrosion attack on stainless steels. According to Ilevbare and Burstein [8], the oxide films have been improved by increasing Ni content in austenitic stainless because its ability to stabilize austenitic phases. In other study, Bilmes *et al*., [9], found that, increasing volume fraction of austenitic phase in stainless steels was improving corrosion resistance behaviour of austenitic stainless steels. However, the microstructure properties of austenitic stainless are detriment when affected with heat sensitization and cooled at slow rate [10]. Sensitization is attributed due the alloy element, degree of temperature and time of heat exposure [11]. The precipitation of $Cr_{23}C_6$ formed when austenitic stainless steels have been exposed for period of time of high temperature and slowly cooled in air [12 – 14]. In addition, Garcia *et al.*, [15] found that, at heat affected zone (HAZ) of welding area, some precipitation of Cr rich carbide developed at intergranular and precipitation of δ-ferrite at transgranular. These precipitations of δ-ferrite and chromium depleted zones were strongly attacked in medium containing chloride anion. Therefore, it shows that heat input was strongly affecting microstructure of materials.

Effect of heat input can influence both detrimental and beneficial effect on the material microstructure which is then directly influencing corrosion resistance of materials. The heat input of welding will cause sensitization (formation of Cr precipitation at grain boundaries) in the HAZ; acceleration of localized attack in the presence of chloride ions [14, 16]. According to Raghuvir [17], corrosion resistance of austenitic stainless steels detriment from classical sensitization when encounter a temperature ranging from 550 to 800 ^{o}C which results in precipitation of chromium carbide along grain boundary with simultaneous depletion of Cr from near grain boundaries. Another finding shows that, appropriate heat input through heat treatment process can bring beneficial effect on microstructure then directly improve corrosion resistance of the material. Candelaria and Pinedo [18] found the corrosion resistance of sensitized stainless steels increased after solution quenching at temperature up to 1100 ^{o}C. It was proved that the increase of austenitizing temperature of up to 1100 ^{o}C promoted the dissolution of carbide and Cr enrichment in matrix. This dissolution increases the retained austenitic phases in stainless steels structure which is promoting beneficial influence on pitting corrosion resistance. The increase of retained austenitic in the structure of stainless steels was improving corrosion resistance attack [9]. Furthermore, secondary recrystallization is more prone in stabilizing austenitic stainless steels [19].

In previous, the effect of the formation and the enrichment of the metallic carbide (i.e., $Cr_{23}C_6$) on the pitting corrosion resistance properties of austenitic stainless steel were debated. However, pitting corrosion behaviour depending on austenitic stainless steel microstructure that particularly developed through the effect of heat input time through preheating of sensitization (by using neutral flame of oxy fuel), and soaking time effect of heat treatment process are yet to be reported.

In this manuscript, the electrochemical technique such as the potentiodynamic cyclic polarization (PCP) measurement was performed to investigate and analyze pitting corrosion resistance properties. Detailed microstructural analyses were also carried out using oxalic acid etching, optical metallurgy microscope and X-Ray Diffraction (XRD). The main aspect of the study is to investigate correlation against pitting corrosion resistance and microstructural features that affected by duration time of heat input in sensitization by blue fire zone of oxy fuel and soaking time of solution quenching. The findings in this manuscript may provide significant information to wide range of industrial

applications; E.g., in desalination engineering industry [20], where American Iron and Steel Institute (AISI) 304 stainless steels has been widely used.

2. EXPERIMENTAL

2.1 Specimen preparation

Wrought AISI 304 stainless steel coupons of 15 mm x 15 mm x 3 mm dimension were used as the specimens. The chemical composition was analysed by using X-Ray Fluorescence (XRF) analysis and the data is shown in Table 1. The surface was mechanically polished with silicon carbide (SiC) paper up to No. 1000 grade and cleaned with distilled water, before the specimens sensitized with neutral flame of oxy acetylene and slowly cooled at room temperature.

Table 1. Chemical composition of AISI 304 stainless steel characterized by XRF.

AISI 304 Stainless Steel	Element (wt. %)						
	Mo	Mn	Ni	Cr	Si	C	P
	0.12	0.80	8.00	18.34	0.64	0.07	0.03

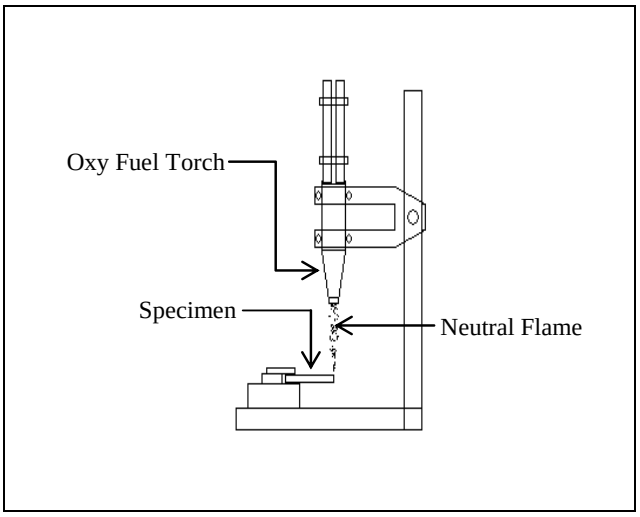

Figure 1. Illustration/scheme of sensitizing process during specimen preparation in this work.

The sensitization was elucidated just at one edge of the specimen. Fig. 1 illustrates sensitization procedure on the specimens. Specimen S0 is the unsensitized (as-received) material specimen. S1 to S5 were marked on sensitized samples that exposed to sensitization for 5 s, 10 s, 20 s, 40 s, and 60 s,

respectively. After the specimens exposed to heat and treated by solution quench, the specimens were repolished for microstructural characterization and corrosion analysis. The sensitized specimens were then treated at temperature 1130 ^{o}C, and soaked at 24, 48, 72, 96, and 120 min and quenched in 15 ± 2 ^{o}C water. This is purposely to dissolve the carbide precipitation. The quenched specimen was marked as Q1 to Q5 for represent specimens treated at soaking 24, 48, 72, 96, and 120 minute respectively.

2.2 Electrochemical measurement

Potentiodynamic Cyclic Polarization (PCP) test was performed using potentiostat (Gamry DC 105) to investigate pitting corrosion properties of sensitized and treated specimens. The exposed surface area of the sample was 3.15 cm^2. 3.5% wt. Sodium chloride (NaCl) solution was prepared following the requirement of American Society for Testing and Materials (ASTM) standard G44 – 99. The test was performed at scan rate of 0.5 mV/s, from -100 mV to +100 mV with respect to the corrosion potential (E_{corr}) and scanning back to the starting potential when the samples reached a current density value of 10^4 μA/cm^2. The counter and reference electrodes were graphite and Ag/AgCl 3 M KCl, respectively. Nobility of pitting corrosion was studied from the hysteresis potential of PCP scan and the pitting nucleation resistance was identified by $E_{pit} - E_{corr}$ of PCP scan [3].

2.3 Microstructural characterization

For electrochemical etching with oxalic acid, ASTM A262 practice A was carried out to determine classification structure of austenitic stainless steels. Then, the etched surface has been examined using optical metallographic microscope. The etched structures have been classified as:

(a) Step structure: No ditches at grain boundaries.

(b) Dual structures: Some ditches at grain boundaries but no single grain completely surrounded by ditches.

(c) Ditch structure: One or more grains completely surrounded by ditch.

Apart from that, austenitic and $Cr_{23}C_6$ phases behaviour were qualitatively analyzed by XRD. XRD analysis was performed at room temperature with PANalytical XPERT PRO MPD PW 3040/60 diffractometer system with monochromatic beam. Data were collected by using Cu-Kα radiation in range $10^0 \leq 2\theta \leq 130^0$ at minimum step interval of 0.001^0.

3. RESULTS AND DISCUSSION

3.1. XRD analysis

Fig. 2 shows the XRD results for unsensitized, sensitized and treated specimens. From the XRD patterns, we suggest the precipitation of metallic carbide $Cr_{23}C_6$ on the sensitized specimens. After solution quenching treatment, the phases of $Cr_{23}C_6$ disappear and the nobility and nucleation pitting corrosion resistance increased in medium containing chloride. Thus, the formation of

precipitation $Cr_{23}C_6$ was strongly detriment the formation of passive layer to resisting corrosion attack in medium containing chloride anion. Such Cui and Lundin [16] found that the precipitation in structure due to sensitization in HAZ was localized attacked in medium containing chloride.

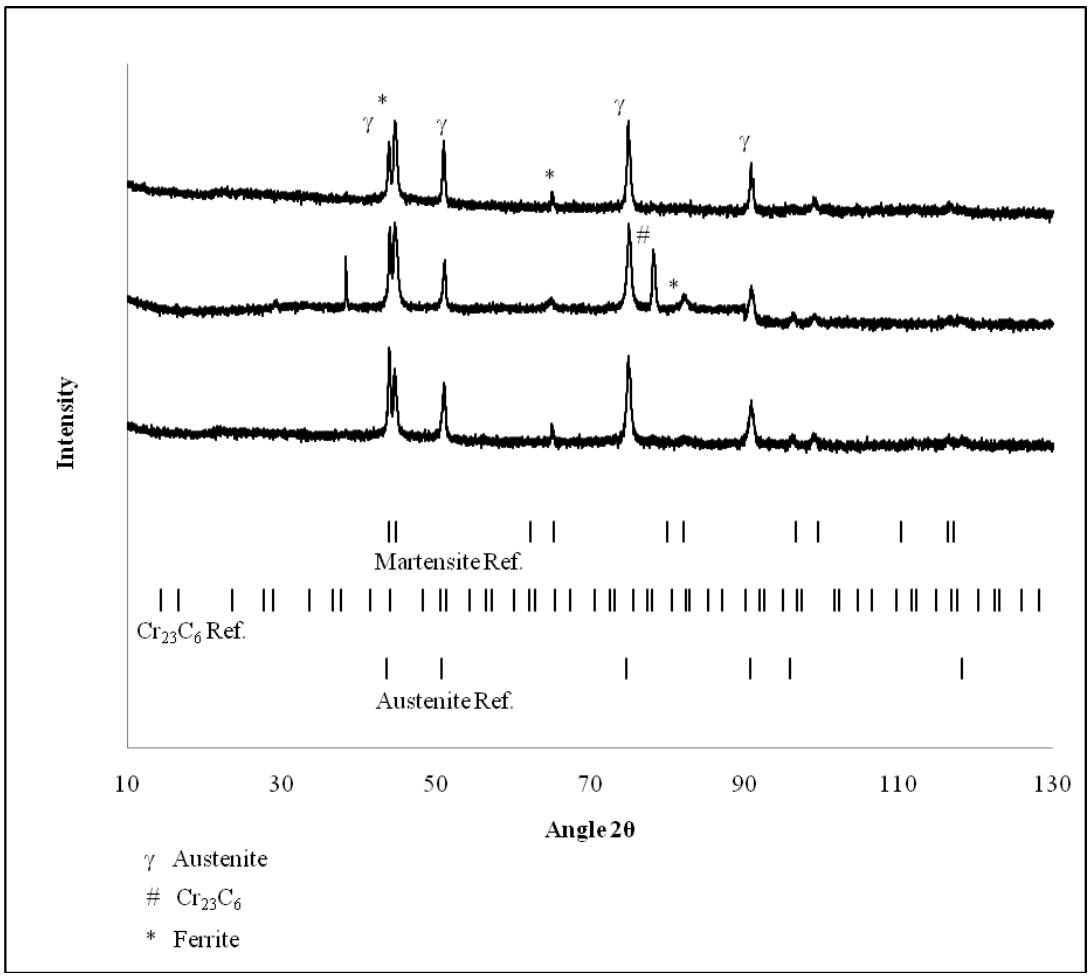

Figure 2. XRD analysis of $Cr_{23}C_6$ in the sequence (from below) of (a) unsensitized, (b) sensitized, and (c) solution quenching treated specimens.

3.2. Microstructural characterization

According to the method of sensitization explained in Experimental, the effect of heat input through the microstructure had been investigated by electrochemical etching with oxalic acid. The precipitation in the sensitized specimens of up to 60 s by neutral flame of oxy acetylene was formed and classified into three zones. Zones of the formation of metallic carbide after sensitized in neutral flame of oxyacetylene are illustrated in Fig. 3.

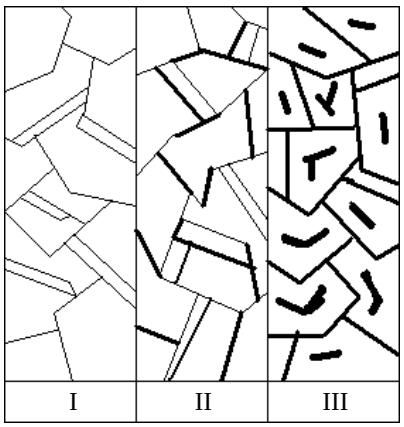

Figure 3. Sketch of microstructure of specimens after sensitization for different zones; Zone I (step structure), Zone II (dual structure & ditch structure), and Zone III (precipitation at intergranular & transgranular).

At the first zone, the step structure which is no precipitation occurs had been observed; the second zone, dual structure which the precipitation had been observed but the grains are not completely surrounded by the precipitation; and the third zone, where directly exposed to the flame of oxyacetylene, ditch structure where the precipitations occur with completely surrounding the grains. Additionally, at the third zone, with increasing of time of the sensitization, the precipitation at transgranular or in the granular of the material had been observed. Further, Fig. 4 shows the percentage area of step structure was reduced due time of sensitization. Here, the precipitation of metallic carbide had been observed. The percentage of step structure was decreasing and is suggested due to the precipitation $Cr_{23}C_6$. The behaviour of the observed microstructure in this study is consistent with the HAZ area of welding on austenitic stainless steels that had been found by Garcia *et al.* [15]; chromium rich carbide developed at intergranular and precipitation of δ-ferrite at transgranular.

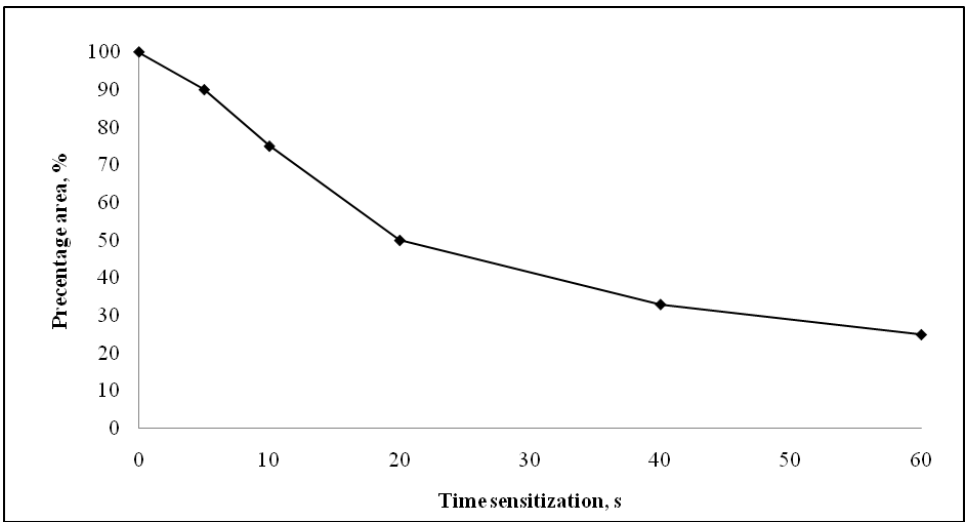

Figure 4. Relation between percentage area of step structure vs. time sensitization.

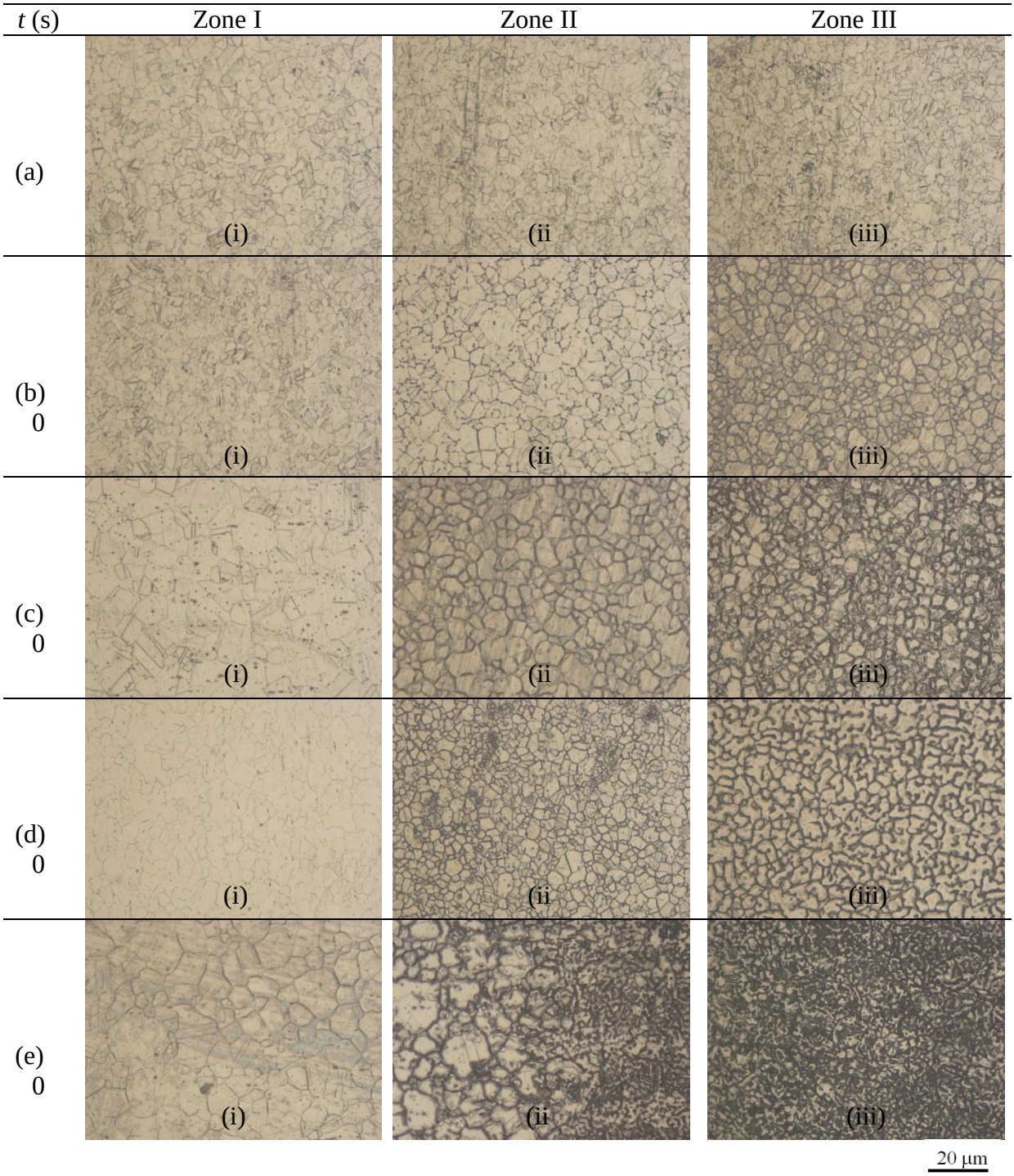

Figure 5. Microstructure behaviour of SUS 304 after sensitized by neutral flame of oxy fuel for (a) 5s, (b) 10s, (c) 20s, (d) 40s and (e) 60s at (i) Zone I, (ii) Zone II and (iii) Zone III. 20x Magnification, scale 20 μm/cm. *Note: Zone I (step structure), Zone II (dual structure & ditch structure), Zone III (precipitation at intergranular & transgranular).*

Fig. 5 shows the microstructure behaviour of sensitized specimens. The enrichment of precipitation at zone II and III increased due to the increasing time of sensitization was observed. The

longer the sensitization time is, the more precipitation detriment the microstructure of austenitic stainless steel [21].

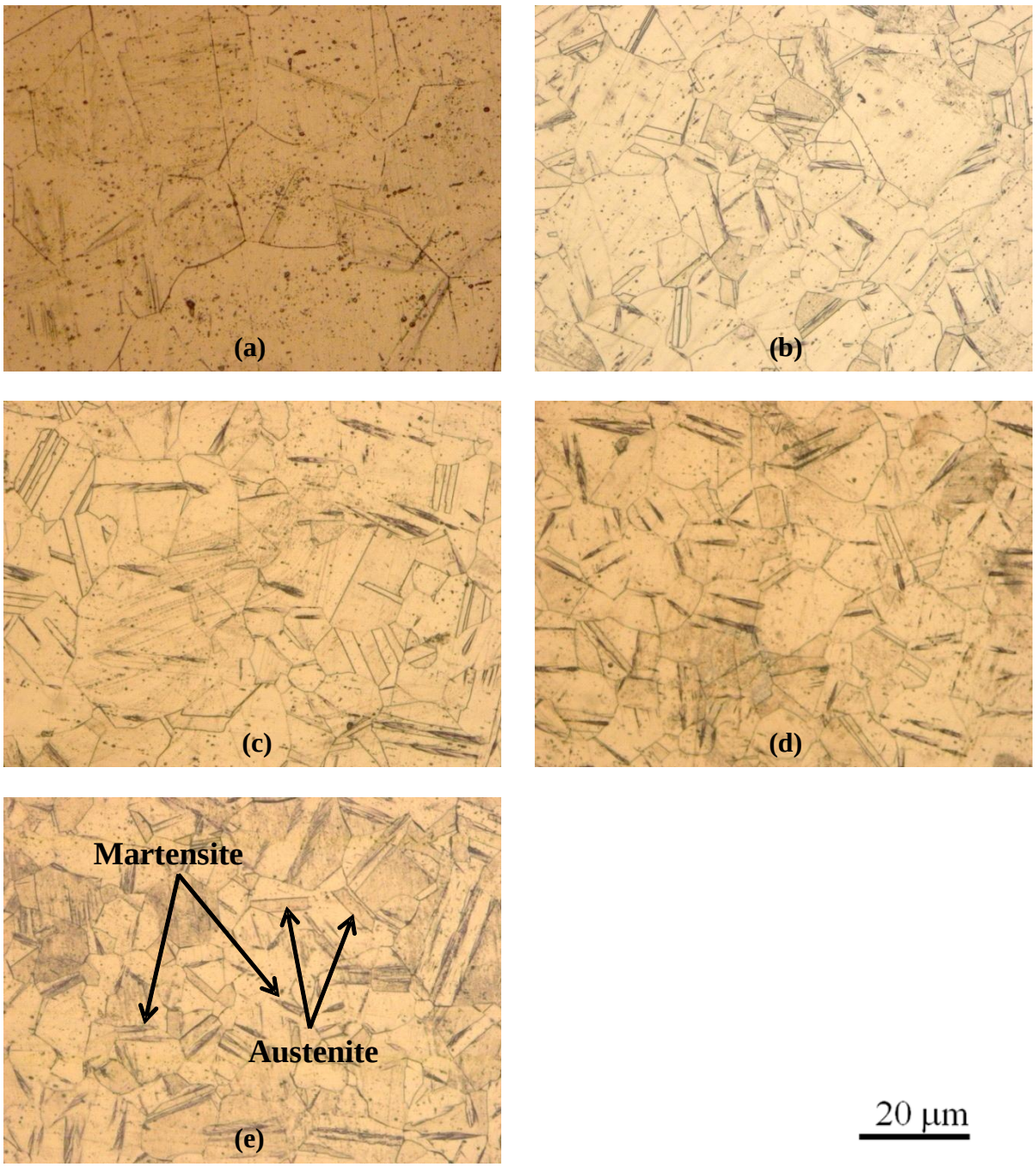

Figure 6. Microstructure behaviour after treatment at 1130 ^{o}C, soaking at (a) 24 min, (b) 48 min, (c) 72 min, (d) 96 min and (e) 120 min, then quenched in 15 ± 2 ^{o}C water. 20x magnification, scale 20 μm/cm.

The detriment of microstructure was caused by $M_{23}C_6$ precipitation and chromium depletion is very frequent in austenitic stainless steels when exposed at high temperature [19]. The heat input and

cooling rate are two important attributes that may affect the microstructure of austenitic stainless steels [15]. We suggest that this can be explained by inducing the segregation of alloying element and the formation of chromium carbide $Cr_{23}C_6$. Therefore, the condition sensitization less than 5 s, it cannot activate the segregation or the diffusion of Cr in the matrix as well to form $Cr_{23}C_6$. Thus, based on the metallographic analysis, only step structure had been observed. After sensitization up to 10 s, dual structure had been observed in zone II and ditch structure at zone III. The precipitation in zone III become worst due to precipitation in grain due to the increasing of sensitization time that mainly associated to the formation of δ-ferrite. The formation of δ-ferrite promotes formation of chromium depleted zone which detriment the austenitic behaviour [15]. Further observation found that, the microstructure at zone III become darker. This condition explained due to formation of coherent precipitation of $Cr_{23}C_6$ [22]. The precipitation metallic carbide and δ-ferrite was dissolved by the solution quenching treatment at temperature 1130 ^oC cooled at cold water 15 ± 2 ^oC. Fig. 6 shows the microstructure of the specimens after solution quenching treatment.

Further observation analysis on metallographic found that, after solution quenching, the martensite structure is formed. The dissolution of $M_{23}C_6$ increases the carbon super saturation and the lattice distortion of the martensite. This condition was promoted by increasing austenitizing temperature up to 1100 ^oC [18]. Thus, formed martensite structure after treatment was a metastable iron phase supersaturated in carbon that is the product of diffusionless transformation from austenite. From the viewpoint of corrosion engineering, the precipitation of $Cr_{23}C_6$ may dissolved in solution annealing treatment which consists of temperature range from 1066 ^oC to 1122 ^oC followed by rapid quenching. Rapid quenching is very important as to ensure the precipitation of $Cr_{23}C_6$ dissolve properly [23]. Thus, it can be suggested that the annealing with rapid cooling gives beneficial effect in which the precipitation had been dissolved.

3.3. Corrosion analysis

Fig. 7 shows the Tafel plot of sensitized specimens through the PCP scan. Tafel extrapolation method is a popular technique to determine corrosion rate of a sample. This correlates to the electrochemical kinetics of an electrochemical reaction to the overpotential. And, Fig. 8 shows the statistical analysis on sensitization time through nobility and nucleation pitting corrosion. Strong correlation between microstructural and pitting corrosion resistance proved that unsensitized structure (classified as step structure) performs low susceptibility to pitting corrosion. The step structure was observed in unsensitized specimens. Unsensitized specimens shows the austenitic structures were perform well in resisting pitting corrosion attack. Fully austenite structure performs good corrosion resistance [7]. However, the precipitation of $Cr_{23}C_6$ was detriment the role of austenitic structure in resisting corrosion attack.

Enrichment of $Cr_{23}C_6$ in the microstructure due to increasing of sensitization time was reducing the nobility and nucleation pitting resistance behaviour of AISI 304 stainless steels specimens in medium containing chloride anion.

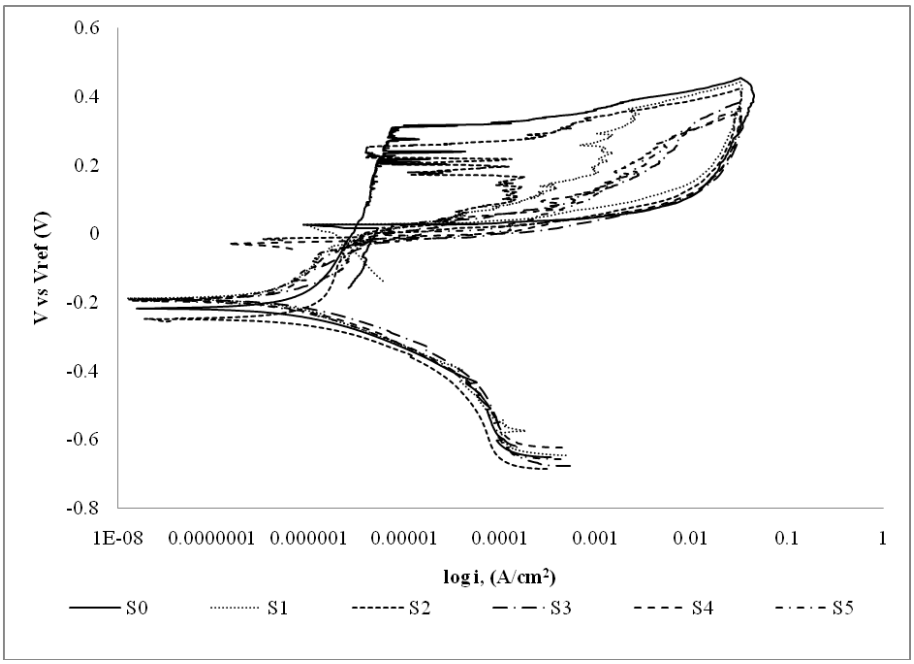

Figure 7. PCP scan analysis on sensitized specimens.

The pitting mechanisms of austenitic stainless steels are always related to the breakdown of the passive film. According to Pardo *et al.*[5], the corrosion resistance of austenitic stainless steels in medium containing chloride is mainly attributed through the enrichment of chromium oxide layer at the metal medium interface. However, the heat sensitization was causing formation of $Cr_{23}C_6$ and depletion of Cr at the adjacent grain boundary [19]. Depleted zone of Cr was localized attacked by medium containing Cl^- [24]. Therefore, the corrosion resistance decreases due to chromium depletion in the adjacent zones to chromium rich precipitates and these precipitations was the causes less stable formation of passive layer. Thus, the depletion of Cr that had been observed is localized attacked in medium containing chloride anion as well reducing the corrosion resistance of the specimens AISI 304 stainless steel.

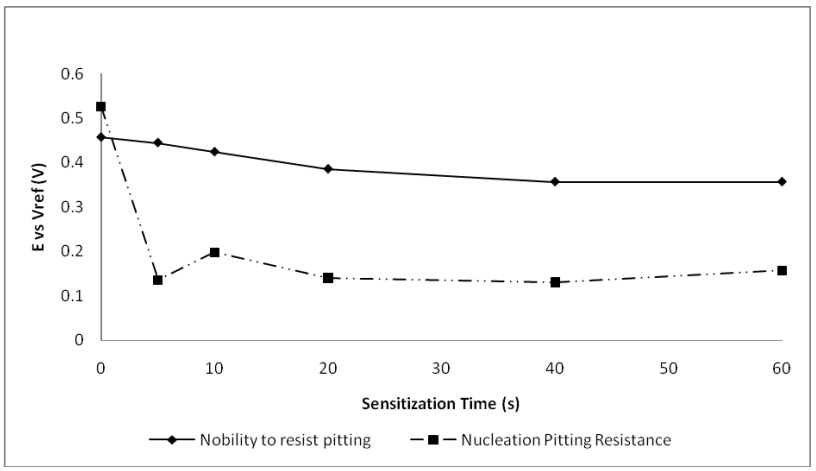

Figure 8. Statistic analysis on pitting resistance behaviour as a function of sensitization time.

Correlating the microstructural behaviour to pitting corrosion resistance behaviour, increasing time of sensitization caused detrimental on the microstructure which directly reduce the pitting nucleation resistance and potential nobility of pitting corrosion resistance. Qualitative analysis on PCP scan shows that, after the specimens sensitized 5 s, the potential value drastically decreased. The next sensitization shows less changes of decrement potential value of nucleation pitting resistance. The nobility potential value of pitting resistance was reduced gradually due to the time of sensitization. It is therefore can be concluded that the passivity and resistance to pitting corrosion were detriment due to the present of $M_{23}C_6$ precipitation.

Next we discuss the PCP scans (Tafel plot) of treated specimens (Fig. 9) and the relation between the nobility to resist pitting and the nucleation of pitting corrosion (Fig. 10). After the precipitation was dissolved by solution quenching treatment, the nobility potential value to pitting corrosion behaviour increased after the sensitized specimen treated at 1130 ^{o}C and soaked 24 min before quench in cold water. Increasing of soaking time up to 48 to 120 min shows the nobility of potential value start to maintain except soaking at 72 min where the nobility potential value decrease slightly. Interestingly, the increasing of treatment soaking time was improving nucleation to pitting corrosion resistance of the. From the PCP scan analysis, the potential value of nucleation pitting resistance increased gradually. Thus, the data shows that, soaking time was the important factor that allowing the transformation to stabilize austenitic structure during treatment. The soaking time promote the diffusion of Cr into the alloy matrix as well as recover austenite structure. Thus the pitting corrosion resistance of sensitized austenitic stainless steels improved due to recovering austenite structure after heat treatment [9].

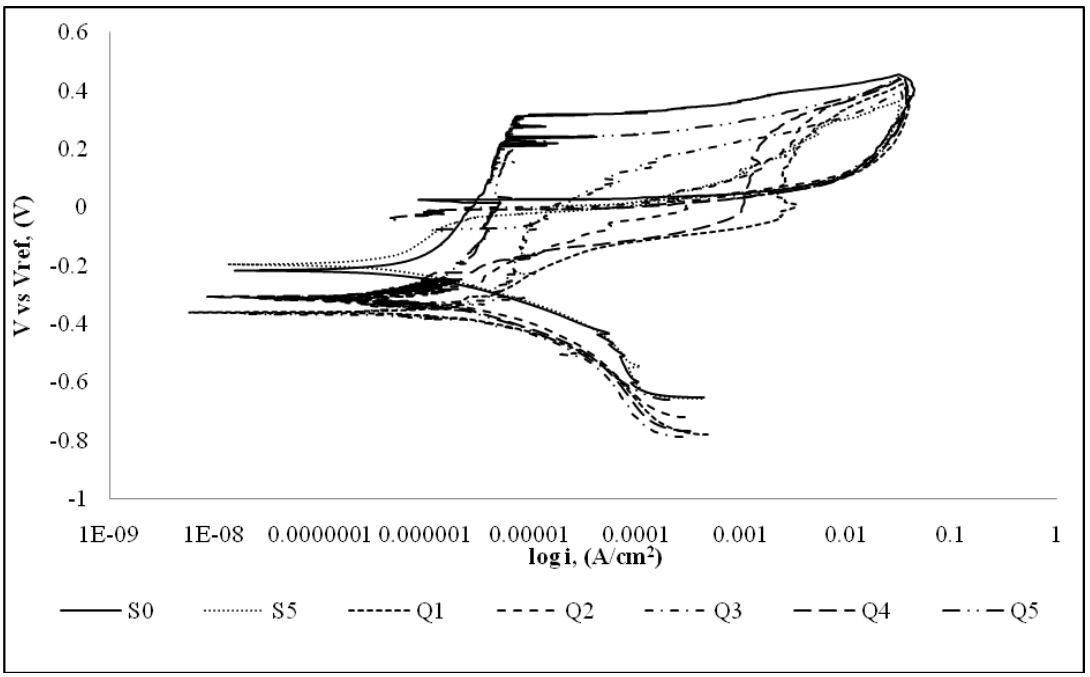

Figure 9. PCP analysis on effect solution quenching treatment soaking time specimens.

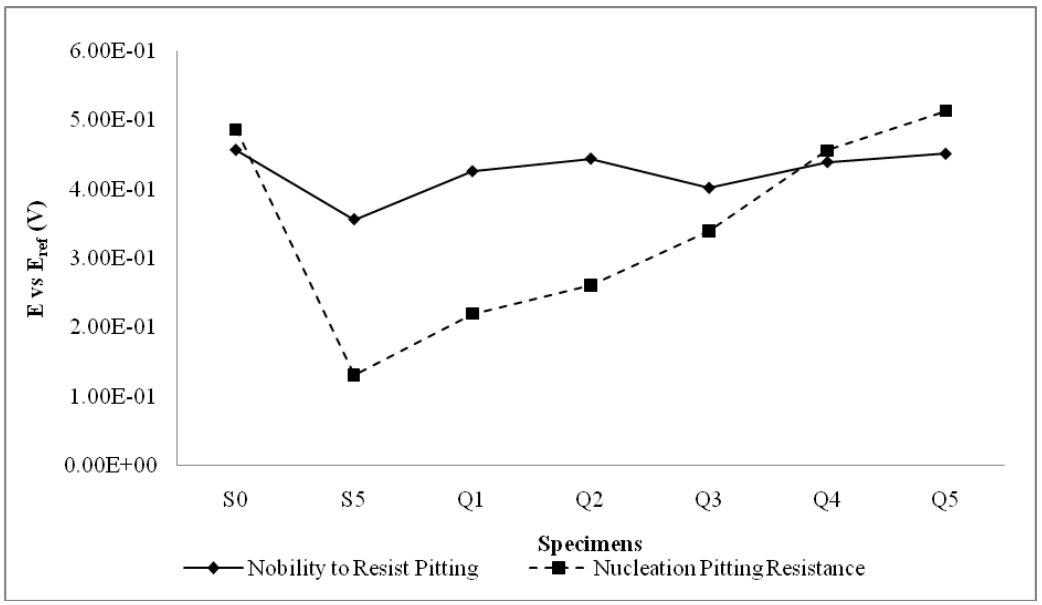

Figure 10. Statistic analysis on effect solution annealing soaking time.

4. CONCLUSIONS

The study on correlation between pitting corrosion resistance and microstructural features that affected by heat input in sensitization has been carried out. From the proposed method of sensitization, XRD analysis confirmed the presence of $Cr_{23}C_6$. The soaking time in heat treatment was an important factor that allowed stabilization of austenitic structure. The microstructure of the sensitized specimens can be classified into three different zones. The enrichment of $Cr_{23}C_6$ in specimens was increased due to the increasing time of sensitization. This enrichment caused the reduction in nobility and nucleation pitting corrosion resistance behaviour of AISI 304 stainless specimens. However, the peak of $Cr_{23}C_6$ disappeared from the XRD pattern after solution quenching treatment. The precipitation had been dissolved due to the solution quenching treatment. The treatment also shows the nobility and nucleation pitting corrosion resistance was improved due to the dissolution of precipitation.

ACKNOWLEDGEMENT
The authors wish to thank Centre of Research and Innovation Management (CRIM), UTeM for the financial support to carry out this investigation through the UTeM Short Term Research Fund No. PJP/2009/FKP(25A)S630.

References

1. M. A. Azam, K. Isomura, A. Fujiwara, and T. Shimoda, *Global Engineers and Technologists Review* 1 (2011) 1 – 8.
2. M. A. Azam, A. Fujiwara, and T. Shimoda, *Appl. Surf. Sci.* 258 (2011) 873 – 882.
3. P. Marcus and I. Olefjord, *Corros. Sci.* 28 (1988) 589 - 602.

4. A. Pardo, M. C. Merino, A. E. Coy, F. Viejo, R. Arrabal, and E. Matykina, *Corros. Sci.* 50 (2008) 780 - 794.
5. A. Pardo, M. C. Merino, A. E. Coy, F. Viejo, R. Arrabal, and E. Matykina, *Corros. Sci.* 50 (2008) 1796 - 1806.
6. B. Jegdic, D. M. Drazic, and J. P. Popic, *Corros. Sci.* 50 (2008) 1235 - 1244.
7. D. J. Lee, K. H. Jung, J. H. Sung, Y. H. Kim, K. H. Lee, J. U. Park, Y. T. Shin, and H. W. Lee, *Mater. Des.* 30 (2009) 3269 – 3273.
8. G. O. Ilevbare and G. T. Burstein, *Corros. Sci.* 43 (2001) 485 - 513.
9. P. D. Bilmes, C. L. Llorente, C. M. Méndez, and C. A. Gervasi, *Corros. Sci.* 51 (2009) 876 - 881.
10. A. Y. Kina, S. S. M. Tavares, J. M. Pardal, and J. A. Souza, *J. Mater Sci.* 5 (2008) 651 - 665.
11. M. Domankova, M. Peter, and M. Roman, *Mater. & Techno.* 41 (2007) 131 - 134.
12. S. Kadry, *Eur. J. of Sci. Research* 22 (2008) 508 - 516.
13. W. E. White, *Mater. Charact.* 28 (1992) 349 - 358.
14. M. Dadfar, M. H. Fathi, F. Karimzadeh, M. R. Dadfar, and A. Saatchi, *Mater. Lett.* 61 (2007) 2343 - 2346.
15. C. Garcia, F. Martin, P. deTiedra, Y. Blanco, and M. Lopez, *Corros. Sci.* 50 (2008) 1184 - 1194.
16. Y. Cui and C. D.Lundin, *Mater. Lett.* 59 (2005) 1542 - 1546.
17. R. Singh, *J. Mater. Process. Tech.* 206 (2008) 286 - 293.
18. A. F. Candelaria and C. E. Pinedo, *J. Mater. Sci. Lett.* 22 (2003) 1151 - 1153.
19. R. L. Plaut, C. D. M. Herrera, P. R. Rios, and A. F. Padilha, *Mater. Research* 10 (2007) 453 - 460.
20. S. A. Al-Fozan and V. A. U. Malik, *Desalination* 228 (2008) 61 - 67.
21. M. Matula, L. Hyspecka, M. Svoboda, V. Vodareka, C. Dagbert, J. Galland, Z. Stonawska, and L. Tuma, *Mater. Charact.* 46 (2001) 203 - 210.
22. M. Shafy, *J. Solids* 28 (2005) 325 - 335.
23. M. G. Fontana, Corrosion Engineering, 3rd Ed. Singapore: McGraw-Hill, 1987.
24. S. S. M. Tavares, V. Moura, V. C. da Costa, M. L. R. Ferreira, and J. M. Pardal, *Mater. Charact.* 60 (2009) 573 - 578.